SEARCHING FOR CORRELATIONS BETWEEN THE STRATOSPHERE TEMPERATURE AND THE COSMIC RAY FLUX AT THE EARTH'S SURFACE

Damián García Castro. Supervised by Juan A. Garzón Heydt, LabCAF, University of Santiago de Compostela
Master's Thesis, September 7th of 2016. Master in Theoretical Physics, Complutense University of Madrid

Preliminary results on the study of correlations between the rates of cosmic rays measured by RPC detectors and the temperature of the atmosphere seem to show that a small detector with good angular, spatial and time resolution would allow to make a prediction of the temperature until almost 50km height. The results discussed in this paper are based on the analysis of two different data samples and it seems that making a good selection in multiplicity, time width, tracks dispersion angle, etc. for each shower, it could be possible to make a prediction of the more likely pressure level where the first interaction has taken place. In addition, several inflection points related to some atmospheric layers have been found but at this moment there has not yet been achieved a reasonable explanation for the position of these points and the study of the contribution of each layer will be necessary in the future.

I. INTRODUCTION

Most of cosmic rays are relativistic charged atomic nuclei, which travel through the space and hit the Earth's atmosphere. They are originated outside the Earth and due to distortions in their trajectories, caused by magnetic fields in the interstellar space, they arrive to the Earth's atmosphere. Around 90% are protons, 9% are alpha particles and the rest is a contribution of medium and heavy nuclei and they are distinguished by their high energies. Most of them have ultrarrelativistic energies that are up to around 10^{20} eV, eleven orders of magnitude greater than the energy of the proton in rest and whose origin is external to our galaxy.

The variations in the cosmic rays flux detected are affected by different effects, as the interplanetary magnetic field induced by the Sun, the solar wind, the Earth's magnetic field or the atmosphere.

II. COSMIC RAYS AND THE ATMOSPHERE

II.A. Extensive Air Showers

Cosmic rays hit the Earth's atmosphere regularly, interacting with atmospheric target nuclei and the subsequent collisions start showers of secondary particles which are called Extensive Air Showers (EAS). The first interaction typically takes place at the altitude between 10 and 30 km, depending on the type of primary particle, and continues until the energy of secondary particles are insufficient to continue the process.

Three major cosmic ray components are distinguished in EAS: electromagnetic, muonic and hadronic. A shower consists in a high energy hadronic core which remain very close to the axis of the shower or the velocity vector of the primary cosmic ray. The hadronic component continually feeds the electromagnetic component producing mesons (mainly pions), which decay in muons, electrons and positrons [1] [2].

The most representative properties of the showers produced by the primary cosmic rays in the upper atmosphere may be summarized in the following parameterizations [3]:

- The time width $\sigma_t(r)$ increases significantly with the distance r to the axis of the shower and is quite independent of the energy of the primary cosmic particle (*Figures 1 and 2*). This behaviour was parameterised by J.Linsley [4] in the form:

$$\sigma_t(r) = \sigma_{t0} \cdot \left(1 + \frac{r}{r_t}\right)^{\beta} \tag{1}$$

where $\sigma_{t0} = 2.6 \;\; ns, \;\; r_t = 30 \;\; m$ and $\beta = 1.5$.

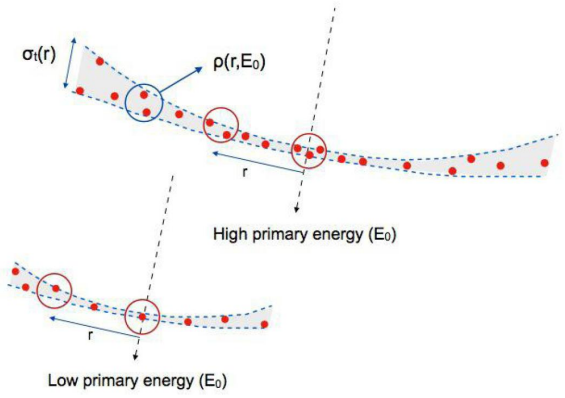

Figure 1: Density of particles and time width as a function of the distance to the center of the shower. High energy showers have bigger densities at comparable distances to the core.

- The density of particles, at a given distance to the core, depends on the number of particles of the shower and the distance in the form:

$$\rho\,(r, N_0) = \epsilon \cdot N_0 \cdot r^{-n} \tag{2}$$

where both, ϵ and n, depend on the mass of the primary cosmic ray. For a proton, $\epsilon = 0.00053$ and $n = 1.5$.

- The energy of the primary cosmic ray is related to the size of the shower by:

$$E_0\left(N_0\right) = \alpha \cdot N_0^b \tag{3}$$

where both, according to A.M.Hillas [5], for a proton $\alpha = 2.217 \cdot 10^{11}$ and $b = 0.798$.

Finally, using equations 1-3, the energy of the primary cosmic ray as a function of the time width and the density of particles measured by a single detector is:

$$E_0 = \alpha \left[\frac{\rho}{\epsilon}\left(r_t\left[\left(\frac{\sigma_t}{b}\right)^{\frac{1}{\beta}} - 1\right]\right)^n\right]^b \tag{4}$$

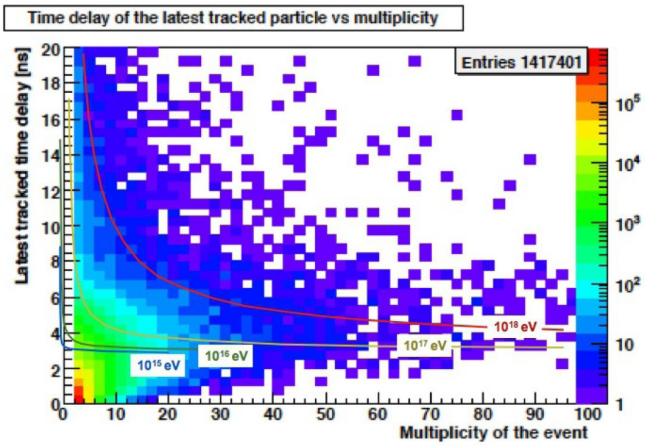

Figure 2: Relationship between the time width and the density of particles observed from the data of HADES experiment.

II.B. The Cosmic Ray Flux and the Temperature of the Stratosphere

The cosmic ray flux registered at the Earth's surface is influenced by the pressure and the atmospheric temperature. The effects of the pressure on the cosmic ray flux are described in the following points:

- If the pressure increases, the density of particles grows too and the particles of the shower suffer more collisions on their way to the surface. Consequently, the total number of secondary particles, detected at the Earth's surface, decreases.
- Whereas, a decrease in the pressure implies a lower density of particles and the total number of secondary particles detected increases.

The temperature of the stratosphere is of special interest and affects to the cosmic ray flux detected at the Earth's surface as follows:

- On the one hand, when the temperature of the stratosphere (above the tropopause, at ~12 km) increases, the density at the air decreases and therefore the interaction probability. A lower density of nuclei in the atmosphere implies that pions have more probability to decay than to interact, producing more high energy muons.This implies that the primary cosmic rays have a greater chance of reaching more depth and the total number of secondary particles, detected at the Earth's surface, grows.
- On the other hand, when the temperature of the stratosphere decreases, the density of nuclei increases and so does the interaction probability. As a result, the first interaction of the primary cosmic rays takes place at higher altitudes and there is a decrease in the number of secondary particles detected at the surface.

The effects described above have been observed in the MINOS experiment, the IceTop array and the IceCube Neutrino Observatory, appreciating the effects of the temperature variations in the muon rate registered.

In the MINOS experiment [6] [7], located underground (720 m) at the Soudan mine (Minnesota, USA), the high energy muon rate ($E_\mu > 0.73$ TeV) was registered during six months (from October to March) every winter between the years 2003 and 2007 and a strong correlation with the effective temperature of the atmosphere was observed (*Figure 3*). This effective temperature was defined as the weighted average that takes into account the distribution of altitudes where the mesons, which decay to the muons detected underground, take place. At those energies of the muons the effective temperature is slightly the same that the upper stratosphere temperature.

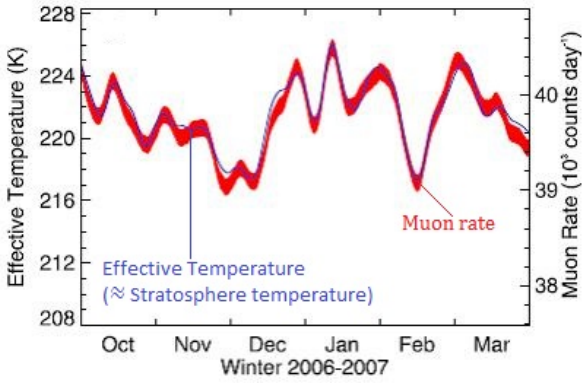

Figure 3: Strong correlation, between the high energy muon rate and the effective temperature of the atmosphere, observed in the MINOS experiment.

Another important experiment in the study of correlations between the muon rate measured and the temperature of the stratosphere has been carried out at the IceCube Neutrino Observatory (South Pole) [8]. The high energy muon rate ($E_\mu \geq 400$ GeV) was registered in IceCube at a depth between 1500-2500 m under ice. The rate detected in IceTop, which is located at the ice's surface, is mostly due to secondary particles with low energy (MeV electrons and gammas, ~1 GeV muons), highly modulated by pressure and temperature.

The time evolution of the temperature of the stratosphere, from May 2007 to April 2009, compared to the flux of particles registered in IceTop and the high energy muon rate observed in IceCube, is shown in *Figure 4*. The yearly temperature variation in the middle stratosphere (20-60 hPa) is highly correlated with the high energy muon rate observed in IceCube and even sudden variations of the temperature can be seen as sudden variations of this rate. However, the counting rates of IceTop have a negative correlation with the temperature in the lower layers of the stratosphere (40-80 hPa).

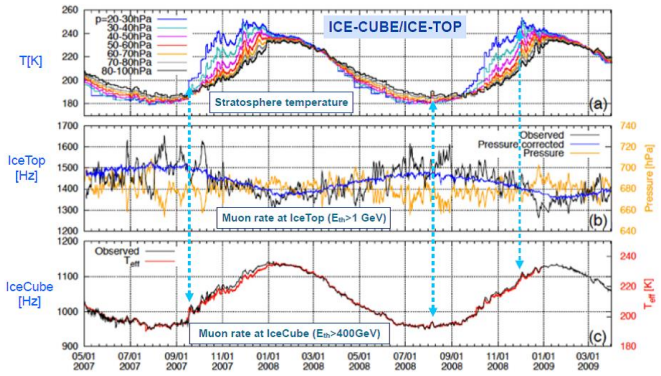

Figure 4: Correlations and anticorrelations observed at IceCube and IceTop, respectively.

The correct interpretation of this arrival information can help us to understand more about the properties of the atmosphere, weather forecasting, global climate change, among many other research fields.

III. INDIRECT DETECTION OF COSMIC RAYS

Cosmic rays with energies above 10^{14} GeV requires indirect detection using big arrays of detectors at the Earth's surface, which is based on the observation of EAS.

The commissioning of the timing RPC-TOF (Resistive Plate Chambers-Time Of Flight) wall of the HADES spectrometer (High Acceptance DiElectron Spectrometer) with cosmic rays, at the GSI (Darmstadt, Germany), opened up the opportunity for a new kind of study about the EAS properties that continues with a new cosmic ray detector at the University of Santiago de Compostela (USC).

III.A. The RPC-TOF Wall of HADES Experiment

The RPC-TOF wall of HADES was designed to optimize the performance of the spectrometer in high multiplicity environments. It covers an area of 7.5 m^2 divided in six sectors (1.25 m^2 each one) of the spectrometer, each one with 187 cells individually shielded of 4-gap timing RPCs distributed in three columns and two planes with trapezoidal shape [3].

Each cell is a entire detector by itself. All of them are packaged into aluminum boxes to electrically insulate from external high frequency signals induced by neighboring cells and to suppress the propagation of the signals registered in each cell with its neighbors. Cells are filled with a Freon-based gas mixture. Two Soda Lime Silicate glass electrodes and three floating aluminum electrodes are used as resistive material in order to generate an electric field inside the gas gaps and to carry the signal from the point at which induces to the exit.

Figure 5: Structure of each sector and setup during the commissioning.

The operation mode of the ionizing gas detectors may be summarized in the following steps:

i) The gas inside the cells are ionized due to the interaction of charged particles that goes through it.

ii) The molecular ions and electrons are dragged to the electrodes and this process could generate an avalanche of charged particles due to the influence of applied electric field.

iii) The unbound ions and electrons produce an induced current in the electrodes that is recorded by acquisition electronics.

iv) Once all charges have been absorbed, the process stops.

During the cosmic ray commissioning of the detector, pairs of two sectors were placed horizontally at a distance of ~35cm as it is shown in *Figure 5*. The resolution for individual cell during the test was 77 ps σ. Cosmic rays were measured making a trigger between at least 1 hit in the upper sector and 1 hit in the lower. The tracks are reconstructed taking into account these hits and looking the trajectories of speed compatible to the speed of light, which allow the determination of the incidence angle of the particle using the *TimTrack* algorithm developed by J.A.Garzón [9].

The possibility of separating the incident particles as a function of the incidence angles allows the study of the different parts of the cosmic ray showers.

III.B. The TRAGALDABAS Cosmic Ray Detector

The systematic analysis of the HADES cosmic ray data has shown several interesting features still not well understood. In order to take their own measures of cosmic rays and to study their properties, the LabCAF research group of the USC in collaboration with other research institutions, has installed a detector called TRAGALBADAS (TRAsGo for the AnaLysis of the nuclear matter Decay, the Atmosphere, the earth B-Field And the Solar activity) at the Faculty of Physics of the USC. This detector is based on RPC technology and is the first of its kind focused on the analysis of cosmic rays using unprecedented high temporal and spatial resolutions. The properties of the EAS induced by high energy primary cosmic rays have never been analysed at the Earth's surface with a high granularity and a time resolution at the 0.1 ns scale detector. With this detector it is expected to get, at the Earth's surface, results that show what has been observed in other experiments at certain depths underground (MINOS experiment at the Soudan mine in Minnesota, USA) underwater and under ice (IceCube/IceTop experiment in the South pole).

TRAGALDABAS is a cosmic ray detector, based on the timing RPC technology offering both high granularity (120 pads/plane; pad size: 130 cm^2) and high time resolution (∼300 ps) together with tracking capability. This new detector is inspired on the RPC-TOF wall of HADES experiment and was installed on the first floor of a two-floor building (260m over the sea level), that will reject part of the electromagnetic component of the showers, for the study of cosmic rays at the Earth's surface. [10] [11].

Figure 6: The TRAGALDABAS detector on his present layout.

In the present layout, the detector is composed by four planes of RPC cells with an external size of 1.285×1.650 m^2 each one, placed horizontally providing an angular resolution about $1.5^o - 2^o$ and a hit efficiency ∼1. Each RPC cell have a two-1mm gap and is placed inside a gas tight metacrilate box, filled flowing freon R134a. The four planes are placed at different heights: 0 cm, 90 cm, 120 cm and 180 cm. The acquisition is triggered by coincidences between at least one hit in the first and one hit in the third plane.

TRAGALDABAS was taking data with coincidence trigger between both planes, at a rate of about 7 million of registered events per day (80 Hz). The TRAGALDABAS Collaboration is formed by a interdisciplinary and international group of scientific researchers and we have the aim to understand better the EAS to go deeper in the relationship between cosmic rays in a broad range of energies and different phenomena related with the Earth's environment.

IV. DATA ANALYSIS

IV.A. Introduction

Differential Temperature Coefficients

The analysis that has been carried out for both HADES and TRAGALDABAS data has focused on the search of correlations between the rate of particles registered at the Earth's surface and the temperatures related to many pressure levels of the Earth's atmosphere. Files of data registered by the two detectors described in the previous section, have been used. On the one hand, with regard to the data sample from the RPC-TOF wall of Hades, we have been provided with a file that allows to study a large number of variables of each coincidence registered by the detector. On the other hand, we have been studied the first unpacked files of the data registered by the TRAGALDABAS. These data have not yet been prepared in the same way and therefore it has not been able to carry out the study as deep as has been done with HADES data. Both data files as well as the development of their analysis are briefly described later in their respective subsections.

To study the behaviour of the different rates with regard to the temperature at different atmospheric layers we have been focused on the calculation of the Differential Temperature Coefficients (DTC), more recently described by A.N.Dimitrieva et al. [12], for each one of the 37 pressure levels that have been used. These coefficients make possible to correct counting rate taking into account the changes of the temperature at all altitudes of the atmosphere. If atmospheric temperature is changed by $\Delta T(h)$ (h is the atmospheric depth in atm) the standard muon flux that arrive with a certain zenit angle (θ) $N_0(E_{min}, X, \theta)$ at observation level X will be changed by $\Delta N_T(E_{min}, X, \theta)$ and the relative change of the muon flux can be written in the following way:

$$\frac{\Delta N_T(E_{min}, X, \theta)}{N_0(E_{min}, X, \theta)} \cdot 100\% = \int_0^X W_T(E_{min}, X, h, \theta) \Delta T(h) dh$$

$$\simeq \sum_i W_T(E_{min}, X, h_i, \theta) \Delta T(h_i) \Delta h_i \qquad (5)$$

where the function $W_T(E_{min}, X, h, \theta)$ is called DTC and can be found on the basis of the formulas describing muon

production and propagation in the atmosphere. In addition, MINOS and IceCube/IceTop results can be explained with these coefficients.

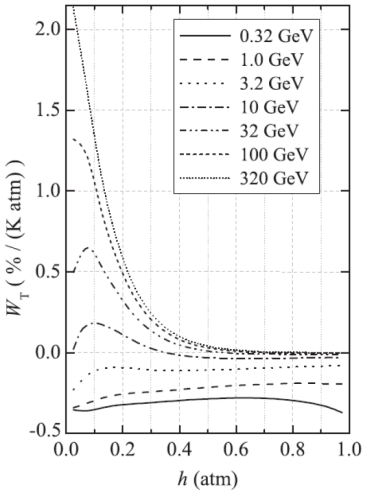

Figure 7: W_T for muons arriving vertically to the sea level with different values of threshold energy as a function of atmospheric deep.

The behavior of the coefficients can be seen in *Figure 7*. The high energy muon flux is very sensitive to the temperature of the stratosphere ($h < 0.2$ atm). In other words, small changes in the temperature of the stratosphere translates into abrupt changes of the high energy muon flux arriving to the ground. On the contrary, the low energy muon flux behaves as opposed to the high energy. This means that when the high energy muon flux at the Earth's surface increases, as a result of the increase in the temperature of the stratosphere, the low energy muon flux decreases. In order to study these effects, the need arises to use a detector capable of measuring the muon flux for different energies that reach the surface along with a model that provides the temperature profiles to measure changes in the stratosphere.

The relationship between muon rates and temperatures of the different pressure levels of the atmosphere has been studied as follows:

$$\frac{\Delta R_\mu}{< R_\mu >} = \alpha_T^p \frac{\Delta T^p}{< T^p >} \tag{6}$$

where α_T^p is the temperature coefficient (equivalent to DTC) for each pressure level, $< T^p >$ is the average temperature for the pressure level p and $< R_\mu >$ is the average muon rate during the period of time under review and $\Delta R_\mu = R_\mu - < R_\mu > \Delta T^p = T^p - < T^p >$. The correlation and temperature coefficients have been calculated by a regresion analysis for each pressure level.

Multivariate Analysis

The multivariate analysis used was based in the methodologies explained by D.Peña [13] and the objective has been to calculate the coefficients that allow us to calculate a prediction of the temperature of the stratosphere. The correlations between all the selected multiplicities or energies and the temperature at different pressure levels give us these coefficients. Our attention have been focused on the variations of these coefficients and its behaviour during the analysed period of time.

The process followed to get the matrices of partial correlation coefficients, may be briefly summarized in the following steps:

i) The first step was the creation of the data matrix ($\mathbf{X}$) which rows were identified with showers and its columns with all the variables that will be analysed for each case.

ii) Creation of the centering matrix ($\mathbf{H}$) with size $n \times n$ where n was equal to the number of rows or time average intervals of the matrices of the different cuts. This matrix is symmetric and idempotent, has $n-1$ range and projects the data orthogonally to the space defined by the constant vector (with all the coordinates equal).

$$\mathbf{H} = \mathbf{I} - \frac{1}{n}\mathbf{1}\mathbf{1}' \tag{7}$$

where $\mathbf{1}$ = (1,...,1)' is the column vector of ones with size $n \times 1$ and $\mathbf{I}$ is the identity matrix $n \times n$.

iii) The next step consisted in the calculation of the variance-covariance matrix ($\mathbf{S}$) using:

$$\mathbf{S} = \frac{1}{n-1}\mathbf{X}'\mathbf{H}\mathbf{X} \tag{8}$$

iv) Calculation of the matrix of correlations between pairs of variables ($\mathbf{R}$), taking into account the contribution of the others, with the next equation:

$$\mathbf{R} = \mathbf{D}^{-\frac{1}{2}}\mathbf{S}\mathbf{D}^{-\frac{1}{2}} \tag{9}$$

where $\mathbf{D}$ is the diagonal matrix with the standard deviation of the variables.

v) Finally, the matrix of partial correlations between pairs of variables ($\mathbf{P}$) was obtained. The direct dependence between two variables, keeping the effect of the others under control, is measured by the partial correlation coefficient.

$$\mathbf{P} = (-1)^{diag}\mathbf{D}(\mathbf{S}^{-1})^{-\frac{1}{2}}\mathbf{S}^{-1}\mathbf{D}(\mathbf{S}^{-1})^{-\frac{1}{2}} \tag{10}$$

where $\mathbf{D}(\mathbf{S}^{-1})$ is the diagonal matrix gotten by selecting the diagonal elements of the matrix $\mathbf{S}^{-1}$ and the term $(-1)^{diag}$ implies a sign change on all the elements of $\mathbf{P}$ except on the diagonal elements.

IV.B. HADES Data Analysis

As it was said in the introduction of this section, the development of several computer programs were carried out in order to do a detailed study of the correlations between the temperature of the stratosphere and the cosmic rays flux detected at the Earth's surface. The first cosmic ray data which have been studied and discussed in this paper come from the commissioning of the RPC-TOF wall of HADES spectrometer with cosmic rays and corresponds to a period of continuous and stable measures between October 14th and 19th of 2009, in which ~40 million of events were detected. Some of the most significant features of the analysed data are the following:

- HADES data collected between October 14th (16h) and 19th (00h)of 2009. A large amount of variables were available to do the analysis: number of hits in the upper and lower planes, number of tracks compatible to the speed of light, their coordinates related to the detector axis, their time of flight, zenit and azimuthal angles, among many others. Subsequently averaged over intervals of six hours.

  It has been made a selection of the most relevant variables for our study and all tracks of the same event have been grouped to analyse each type of shower individually. As a result of this grouping, standar deviation (σ_t), skewness and kurtosis of the time of flight have also been calculated. The most relevant properties discussed in this paper are σ_t, the multiplicity of a shower which is related to the number of hits detected on the upper plane and its energy that has been estimated using equation 4.

- Atmospheric data registered every six hours at the nearest weather station to Darmstadt. This include temperature and geopotential values for 37 pressure levels: 1, 2, 3, 5, 7, 10, 20, 30, 50, 70, 100, 125, 150, 175, 200, 225, 250, 300, 350, 400, 450, 500, 550, 600, 650, 700, 750, 775, 800, 825, 850, 875, 900, 925, 950, 975, 1000 hPa.

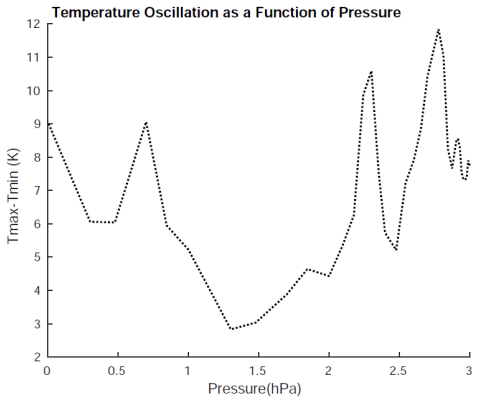

Figure 8: Temperature oscillation ($T_{max} - T_{min}$) for each pressure level during the five days studied.

In the first place, for the different cuts that have been made with respect to the σ_t value (< 0.5, < 1, < 2 and < 5 ns), we have chosen different ranges of multiplicities M (M=1, M=2, LM (2<M<9) and HM (M≥10)). In addition, there have been prepared cuts for preliminary energies calculated by equation 4 (E1: $10^{13} - 10^{14} eV$, E2: $10^{14} - 10^{15} eV$, E3: $10^{15} - 10^{16} eV$ and E4: $> 10^{16} eV$). Taking into account equation 6, it has been studied the behaviour of the relative variation of muon rate as a function of the relative variation of temperature for all pressure levels. In this way, we have determined the values of the correlation coefficients between both variables as well as the values of the slopes resulting of the linear regresion.

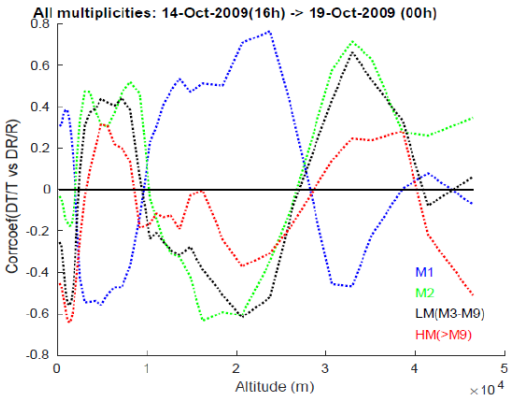

Figure 9: Correlation coefficients of the linear regresion explained above for different altitude levels, all multiplicities and $\sigma_t < 1$ ns.

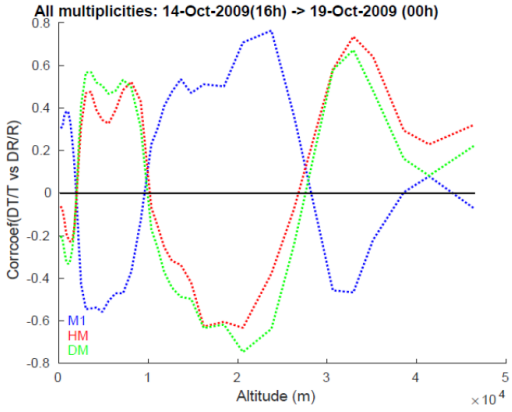

Figure 10: Correlation coefficients of the linear regresion for different altitude levels and $\sigma_t < 1$ ns, but now only for multiplicities M1, $M > 1$ and their ratio (DM).

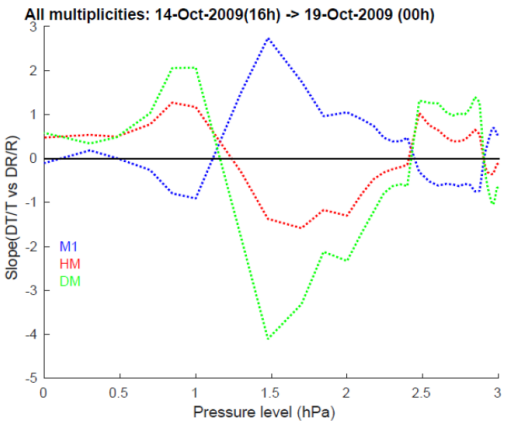

Figure 11: Slopes of the linear regresion for the pressure levels (logarithmic scale) and $\sigma_t < 1$ ns for M1, $M > 1$ and their ratio (DM).

In the previous figures, there have been observed several behaviours that require a more detailed description. In *Figure 9* one can see the variation of the correlation coefficient for all multiplicities, resulting from the linear regresion (equation 6), as a function of altitude. *Figures 10 and 11* show the same but working only with two ranges of multiplicity (M1 and $M > 1$ due to the low statistics for high multiplicities) and its ratio for both altitude and pressure levels. It seems that there are *four inflection points* for both correlation coefficient and slope which are apparently related to the following layers of the atmosphere:

- 0-2.5km: Correlation between rate of M1 and temperature. This layer is associated with low cloud formation and temperature oscillations ($T_{max} - T_{min}$) are small.
- 2.5-10km: Correlation between rate of $M > 1$ and temperature. Middle and high cloud formation takes places at this altitudes and temperature fluctuations are higher.
- 10-27km: Correlation between rate of M1 and temperature. Temperature oscillations are too small except in the tropopause, at $\simeq$12km. The increase in M1 seems to indicate that most of the secondary cosmic rays detected have been originated in that area which is where nuclear collisions produces the maximum of particles.
- 27-42km: Correlation between rate of $M > 1$ and temperature. The highest ozone concentrations are located here and temperature variations increases to higher values.
- 42-50km: Rate of M1 and $M > 1$ have a similar behaviour with temperature. At these altitudes it seems that is where the first interaction of the primary cosmic rays with atmospheric nuclei takes place.

The analysis that has been described for multiplicities also has been done for energies. In this development, energies have been grouped in two intervals for the same reason that in the case of multiplicities. These ranges are: LE ($10^{13} - 10^{14} eV$) and HE ($> 10^{14} eV$) for which the contribution of M1 events has been removed due to not be able to calculate its energy by equation 4. *Figures 12 and 13* show the behaviour of LE, HE and their ratio (DE) for different altitude and pressure levels. In contrast to the results described in the first case, now one can see only a single inflection point which corresponds to the tropopause. Below 12km effects of temperature variations mostly affect low energy events. In contrast, for altitudes above 12km the behaviour is the opposite and begin to dominate the effects on high energy events.

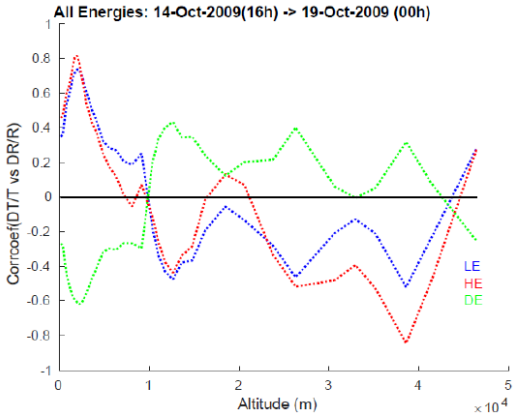

Figure 12: Correlation coefficients of the linear regresion explained above for altitude levels.

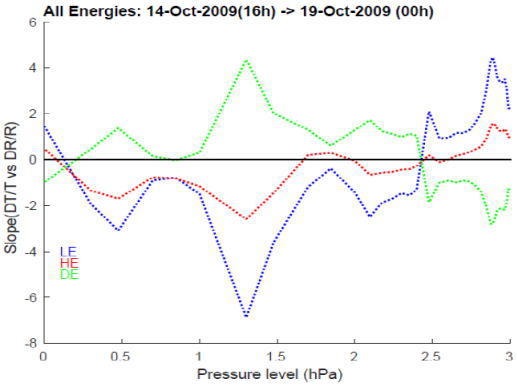

Figure 13: Slopes of the linear regresion for the pressure levels (logarithmic scale).

Temperature estimation

Finally, using the rates of all intervals for both multiplicities and energies as well as the temperatures for altitude and pressure levels, we have proposed as objective to give an estimation of the temperature for each one of the atmospheric layers. This has been carried out using the multivariate analysis techniques described in the introduction of this section. The study has been done by including in the multivariate analysis the values of all intervals of six hours except those corresponding to the two central points of time interval available. In this way, the values of the coefficients that take into account the contribution of each one of the four multiplicities. It has been done only for two points due to the few days of available data. The aim is to extend it to longer periods of time and make a prediction of the temperature in the medium term. In addition, it has been repeated for the four energy intervals getting comparable results as can be seen in *Figures 14 and 15*. The coefficients obtained allow us to give a prediction of the temperature for the two central six hour intervals using the following equation:

$$T_{pred} = b_0 + b_1 X(:,2) + b_2 X(:,3) +$$

$$+ b_3 X(:,4) + b_4 X(:,5) \qquad (11)$$

where **X** is the matrix in which rows were identified with the showers and the columns with the multiplicities or energies.

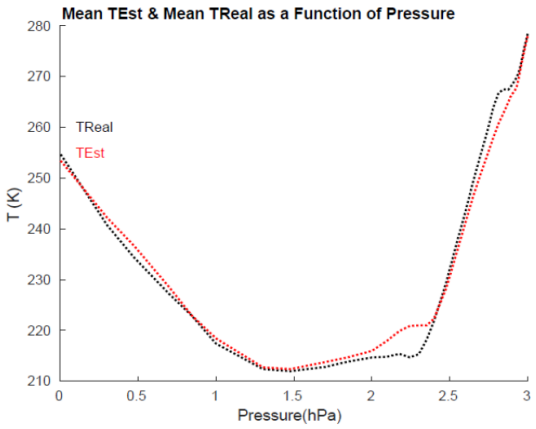

Figure 14: Temperature prediction (red) vs measured (black) as a function of the pressure levels (logarithmic scale) using multiplicities and averaged for the two central six hour intervals.

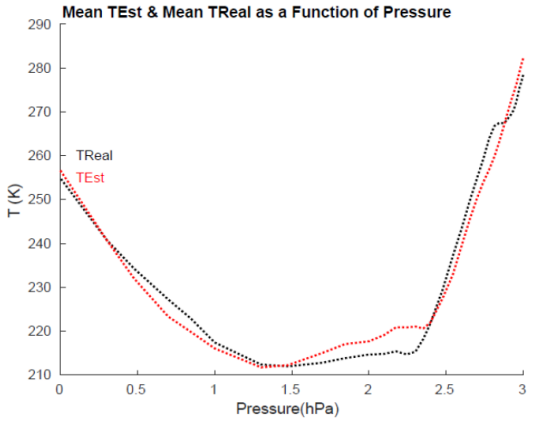

Figure 15: Temperature prediction (red) vs measured (black) as a function of the pressure levels (logarithmic scale) using energies and averaged for the two central six hour intervals.

In summary, correlations and anticorrelations between different rates of cosmic rays registered and the temperature of the atmosphere have been studied. There have been found several behaviours associated with different layers of the atmosphere. The influence of each one them on the rate of particles detected at the Earth's surface still not understood but it will be an object of study in the near future. In this way, we will be able to explain why in some areas the effects of temperature on M1 (or LE) dominate while in others the effects on $M > 1$ (or HE) are the dominant, as well as to do a better study of the inflection points observed.

Another important result is that we have managed to establish a new unprecedented way to predict the temperature as a function of the rate of cosmic rays. Both studies show a very good estimation for all pressure levels in comparison with the real measured temperature except for those areas in which the variation of temperatures with regard to their average value has been higher (∼2.5 and 12 km).

IV.C. TRAGALDABAS Data Analysis

In order to a better understanding and to be able to explain acccurately the results that have been seen for the HADES data, other analysis are necessary. For this reason, we have analysed a second cosmic ray data which come from the first unpacked cosmic ray data files of the TRAGALDABAS detector. The analysis described in this subsection is similar to that described for the HADES data. Some of the most significant features of the analysed data are the following:

- TRAGALDABAS data collected between April 1st (00h) to October 1th (00h) of 2015. Unlike the data sample described in the previous subsection, the data file from the TRAGALDABAS has not allowed us to do a detailed study because we only had the rates of unambiguous events with multiplicity 1 (M1), 2 (M2) and 3 (M3). That is to say, events with one, two or three tracks compatible with the speed of light. As a consequence, it has not been possible to define cuts as a function of σ_t, multiplicity or energy. These data have been rebuilt for two of the four detector planes and in the near future the first files of data taking into account three of them will be available. Despite not having a large amount of information as in the previous sample we have analysed different periods of seven days for all months except August due to some problems with the acquisition data.

  We have chosen several weeks with different weather conditions mainly distinguished between stable and unstable (high humidity, rain and wind speed) weeks. The data were subsequently averaged over intervals of six hours.

- Atmospheric data registered every six hours and downloaded from the reanalysis database ERA-INTERIM. The temperature profiles at the TRAGALDABAS location have been obtained by averaging the nearest 9 points of the mesh. This include temperature and geopotential values for the same 37 pressure levels as in the previous discussion.

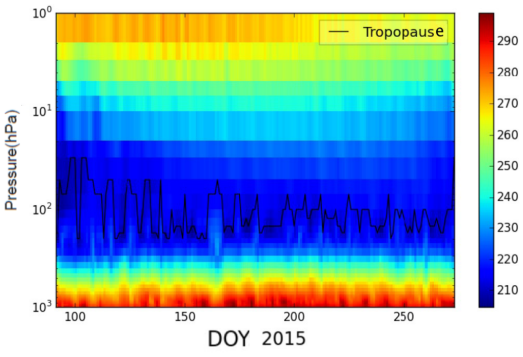

Figure 16: Temperature variation for the pressure levels (logarithmic scale) and the tropopause position between April 1st to October 1th of 2015.

Irma Riádigos in her master's thesis [14] has studied the evolution of temperature coefficients α_T^P obtained from the linear regresion to the equation 6 for different altitude levels (*Figure 17*). Her studies have been made using daily averages of both rates and temperatures values along the 6 months of available data. Although the values of α_T^P were very small due to the bad fitting caused by the great dispersion, it is very important to observe the general behaviour. One can see the correlations or anticorrelations for the three multiplicities in different layers of the atmosphere.

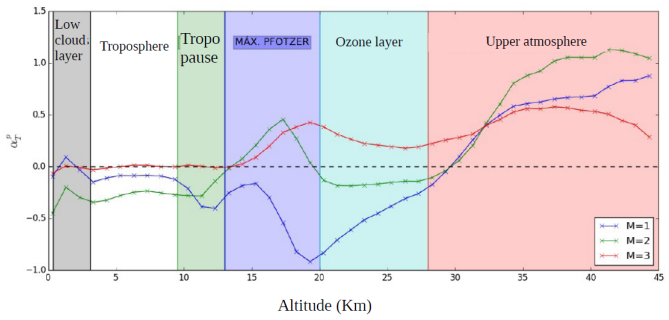

Figure 17: Evolution of the α_T^P coefficient for each one of the three multiplicities as a function of altitude levels.

Next figures show some of the results obtained concerning correlation coefficients and slopes of the fitting between the relative variations of rates and temperatures for $M1$, $M2+M3$ (multiplicities 2 and 3 have been grouped) and their ratio (DM).

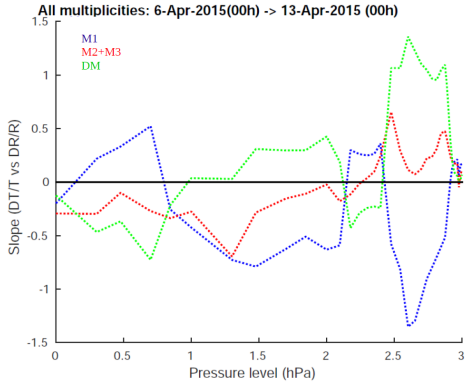

Figure 18: Slopes for the pressure levels (logarithmic scale) from April 6th to 13th.

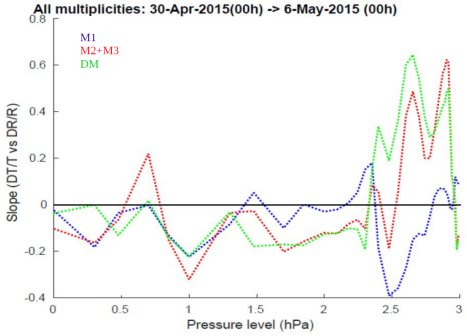

Figure 19: Slopes for the pressure levels (logarithmic scale) from April 30th to May 6th.

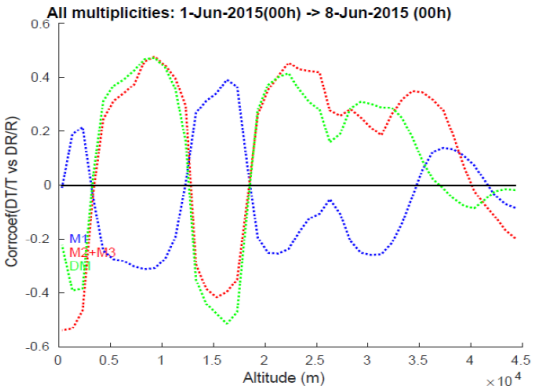

Figure 20: Correlation coefficients for altitude levels from June 1st to 8th.

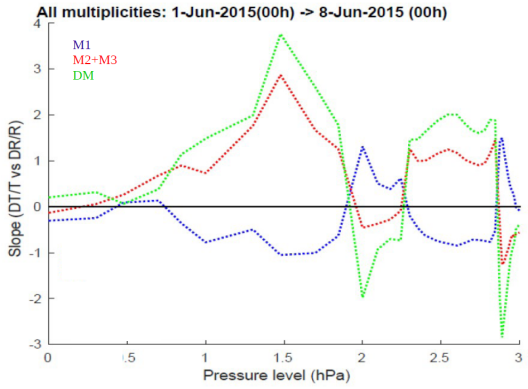

Figure 21: Slopes for the pressure levels (logarithmic scale) from June 1st to 8th.

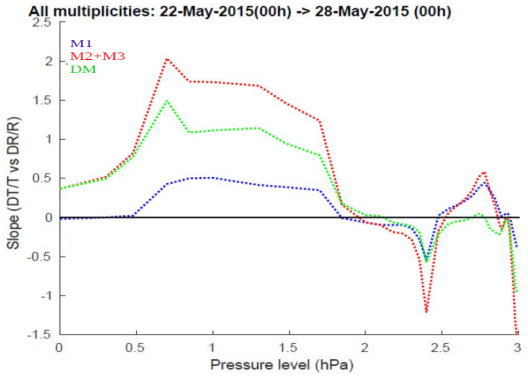

Figure 22: Slopes for the pressure levels (logarithmic scale) from May 22th to 28th.

In spite of the fact that the observed behaviour is very clear, we have studied its stability for weekly periods of cosmic ray data and the results are diverse.

In summary, the behaviors that have been seen change for some weeks while for others the inflection points observed are located at the same layers that have been identified with HADES data. The results are not conclusive yet but although there is a promising method it is necessary to do a more detailed analysis. Everything seems to indicate that this method works for days of great stability but we have to be cautious with larger periods of unstable days because it may fail.

V. CONCLUDING REMARKS

In order to carry out a concise and detailed analysis of the correlations between the cosmic ray flux measured at the Earth's surface and the temperature of the stratosphere, it has been carried out the development of several tools. This process has been performed using the cosmic ray data sample from the commissioning period of the RPC detectors of HADES experiment and the first unpacked cosmic ray data from the TRAGALDABAS detector.

The inflection points that have been observed for both HADES and TRAGALDABAS seem that are located at confluence areas of different layers of the atmosphere. At the moment there has not yet been achieved a reasonable explanation for the position of these points and the study of the contribution of each layer will be necessary in the future.

In addition, the study of the averaged rates of cosmic rays for different cuts in multiplicity and time width ($\sim$ ns) allow the estimation of the temperature of the atmosphere until almost 50 km height. In fact, direct estimation in real time of the temperature of the atmosphere over the vertical of a place could allow a better prediction of showers propagation which are induced by high-energy cosmic rays. Likewise, it would be possible to improve the estimation of its energy, mass and arrival direction.

Although the results for the HADES data are not yet conclusive due to the fact that they only contain four days of data in which temperature variations were not very high. With a small detector of high multiplicity and angular resolution at the Earth's surface we have been able to check and go deep to the effects that had already been observed both in MINOS and IceCube/IceTop. It is very important to emphasize that in contrast to the results of these experiments, which measures have been taken for several months, the HADES data sample only covered 4 days. However, it is possible that for a greater number of days in which the atmosphere have many temperature changes or turbulences, the study will be more complicated and we need to do more sophisticated studies. For this reason it is necessary to have a sample of the data good enough to allow the study of a large number of variables.

A hypothetical reflection that could be done is: making a selection in multiplicity, time width, tracks dispersion angle, etc. for each shower, we may be able to make a prediction of the more likely pressure level where the first interaction has taken place. For this altitude the correlation between the selected events and the temperature at this height could be maximum.

In any case, we have opened a immense line of work. Correlations with the temperature had already been seen for the stratosphere but not for the lower layers of the atmosphere.

References

[1] Gaisser, T.K. (1990). *Cosmic rays and particle physics.* Cambirdge University Press.

[2] Grieder, P.K.F. (2001). *Cosmic rays at Earth: researcher's reference manual and data book.* 1st edition. Elsevier B.V., Amsterdam.

[3] Korkanov, G. (2012). *New advances and developments on the RPC-TOF wall of the HADES experiment at GSI.* PhD thesis. University of Santiago de Compostela.

[4] Linsley J. (1985). *Mini and super mini arrays for the study of highest enregy cosmic rays.* Proceedings 19th ICRC, 434.

[5] Hillas, A.M. (1975). *Some recent development in cosmic rays.* Phys. Rep. C. 20, 79.

[6] Adamson, P. et al. (2010). *Observation of muon intensity variations by season with the MINOS far detector.* arXiv:0909.4012v3 [hep-ex]

[7] Osprey, S. et al. (2009). *Sudden stratospheric warmings seen in MINOS deep underground muon data.* Geoph. Res. Lett., Vol. 36, L05809.

[8] Tilav, S. (2010). *Atmospheric variations as observed by IceCube.* arXiv:1001.0776v2 [astro-ph.HE].

[9] Garzón, J.A. and Cabanelas, P. (2012). *A matrix formalism for a fast time and track reconstruction with timing detectors.* Nucl. Instr. and Meth. A, 661:s210-s213

[10] Garzón, J.A. et al. (2014). *TRAGALDABAS: a new RPC based detector for the regular study of cosmic rays.* IOP Publishing Ltd and Sissa Medialab srl doi:10.1088/1748-0221/9/09/C09027.

[11] Garzón, J.A. et al. (2012). *Análisis del entorno terrestre mediante un detector de rayos cósmicos con muy alta resolución temporal.* Journal/Editor.

[12] Dimitrieva, A.N. et al. (2010). *Corrections for temperature effect for ground-based muon hodoscopes.* Astroparticle Physics, Volume 34, Issue 6, p. 401-411. Elsevier B.V. doi:10.1016/j.astropartphys.2010.10.013

[13] Peña, D. (2002). *Análisis de datos multivariantes.* McGraw-Hill, Madrid.

[14] Riádigos, I. (2016). *Medida de la temperatura de la estratosfera mediante un detector de rayos cósmicos de alta resolución.* Master's thesis, University of Santiago de Compostela.